

## Electronic Supplementary Information for

# **Single-crystal superprotonic conductivity in an interpenetrated hydrogen-bonded quadruplex framework**

Mu-Yang Zhou, Hao-Yu Wang, Zhi-Shuo Wang, Xue-Wen Zhang, Xi Feng, Le-Yao Gao, Zhi-Cheng Lian, Rui-Biao Lin, and Dong-Dong Zhou\*

*MOE Key Laboratory of Bioinorganic and Synthetic Chemistry, School of Chemistry, Sun Yat-Sen University, Guangzhou 510006, P. R. China*

\*E-mail: [zhoudd3@mail.sysu.edu.cn](mailto:zhoudd3@mail.sysu.edu.cn)

## EXPERIMENT SECTION

**Materials and Physical Measurements.** Reagents and solvents were commercially available and were used without further purification. Infrared spectra were obtained from KBr pellets on a Bruker Tensor 27 FT IR spectrometer in the 400–4000  $\text{cm}^{-1}$  region. Elemental analyses (C, H, N) were performed with a Vario EL elemental analyzer. Powder X-ray diffraction (PXRD) patterns were recorded using a Bruker D8 ADVANCE X-ray powder diffractometer ( $\text{Cu-K}\alpha$ ). Thermogravimetric analyses were performed using a TA Q50 instrument with a heating rate of 5.0  $^{\circ}\text{C min}^{-1}$  under nitrogen. Scanning electron microscopic (SEM) images were obtained by Hitachi SU8010 apparatus working at an acceleration voltage of 5 kV.

Synthesis of  $(\text{H}_3\text{O})[\text{K}(\text{H}_2\text{imdc})_2(\text{H}_3\text{imdc})_2] \cdot 2.5\text{H}_2\text{O}$  (**1-H<sub>2</sub>O**). A mixture of KOH (5.6 mg, 0.1 mmol), 1*H*-imidazole-4,5-dicarboxylic acid ( $\text{H}_3\text{imdc}$ , 62.5 mg, 0.4 mmol), MeOH (0.5 mL) and  $\text{H}_2\text{O}$  (0.2 mL) was sealed in a Pyrex glass tube and kept at 140  $^{\circ}\text{C}$  for 3 days, then cooled to room temperature at a rate of 10  $^{\circ}\text{C h}^{-1}$  to form colourless rod-like crystals (yield: ~60%). EA calcd (%) for  $(\text{H}_3\text{O})[\text{K}(\text{C}_2\text{H}_3\text{O}_4\text{N}_2)_2(\text{C}_2\text{H}_4\text{O}_4\text{N}_2)_2] \cdot 2.5\text{H}_2\text{O}$ : C, 33.11; H, 3.06; N, 15.44. Found: C, 32.79; H, 2.60; N, 15.64. IR ( $\text{cm}^{-1}$ ): 3700–3400(br), 3169(m), 3087(w), 2980(m), 1983(m), 1730(s), 1629(s), 1531(s), 1451(m), 1385(s), 1241(m), 1202(m), 1084(m), 1037(m), 957(m), 842(m), 774(s), 630(s), 520(s).

**Single Crystal X-ray Diffraction (SCXRD) Structure Determination.** Diffraction data was collected on a Rigaku XtaLAB P300DS single-crystal diffractometer by using graphite monochromated  $\text{Cu-K}\alpha$  radiation. Absorption corrections were applied by using multi-scan program *CrysAlisPro*. The structure was solved with the direct methods and refined with a full-matrix least-squares technique with the SHELXTL program package. Anisotropic thermal parameters were applied to all non-hydrogen atoms. The hydrogen atoms banding on to the O or N atoms of the host framework were found from the nearby Q peaks, and others were generated by the riding mode. Because the solvent guests and counter cations are disordered, which is difficult to confirm the contents of guests, PLATON SQUEEZE treatment was applied to the structure to calculate the electrons. The numbers of squeezed electrons are 152 per unit-cell, which is identical with the current molecular unit (144 per unit-cell). The crystal data as well as the detailed refinements for the structure are summarized in Table S1. CCDC 2114806 contain the supplementary crystallographic data for this paper. The data can be obtained free of charge from The Cambridge Crystallographic Data Centre via [www.ccdc.cam.ac.uk/data\\_request/cif](http://www.ccdc.cam.ac.uk/data_request/cif).

**Impedance Analyses.** Pellets with 5 mm in diameter and 0.4–0.9 mm thick were prepared by pressing microcrystal samples at 780 MPa and carefully glued with Pt wires using conductive silver paste. The facets of the selected single crystals were indexed by a Rigaku XtaLAB P300DS single-crystal

diffractometer and carefully glued with Pt wires using conductive silver paste. The alternating current (ac) impedance measurements were performed using the conventional two-probe method with an impedance and gain-phase analyzer (Solartron SI 1260 Impedance/Gain-Phase analyzer) over frequency range 1 Hz – 10 MHz with an input voltage amplitude of 200 mV under different humid conditions (controlled by using an SMA–2UF incubator). Each conductivity measurement was performed after waiting for 8 hours at the target condition (temperature and relative humidity). The software ZView2 was used to fit impedance data sets by means of an equivalent circuit simulation to obtain the resistance values. The resulting response was displayed in the form of a Nyquist plot. The proton conductivity ( $\sigma$ , S cm<sup>-1</sup>) was calculated by the following equation:  $\sigma = L/RA$ , where  $\sigma$  is proton conductivity in S cm<sup>-1</sup>,  $L$  (cm) is the thickness of the sample,  $A$  (cm<sup>2</sup>) is the area available for proton conduction, and  $R$  ( $\Omega$ ) is the real part of the impedance value obtained from the equivalent circuit simulation. Activation energy ( $E_a$ , eV) for the conductivity was estimated from the following equation:  $\ln(\sigma T) = -E_a/k_B \times 1/T + \ln(\sigma_0)$ , where  $\sigma_0$  is the pre-exponential factor,  $k_B$  is the Boltzmann constant and  $T$  is the temperature (K). The final presented conductivity was the averaged value of conductivities from three single crystals or pellets.

**Computational Simulations.** All simulations/calculations were performed using the Materials Studio 5.5 package. Firstly, the model of the host framework was constructed from the single-crystal structure of **1**, but the hydrogen atoms of imidazole moiety were considered to be ordered by decreasing the crystal symmetries from  $I4_1/a$  to  $I4_1$ , and the structure was optimized through density functional theory (DFT) in the Dmol<sup>3</sup> module. The preferential sorption sites of H<sub>3</sub>O<sup>+</sup>/H<sub>2</sub>O were simulated by grand canonical Monte Carlo (GCMC) with fixed loading operations. The simulation box consisted of 1 × 1 × 3 unit cells and the metropolis method based on the universal force field (UFF) was used. Mulliken and ESP charges calculated from DFT were adopted to the framework and the guest molecules, respectively. The cutoff radius was chosen as 18.5 Å for the LJ (Lennard–Jones) interactions, and electrostatic interactions and van der Waals interactions were handled using the Ewald and Atom based summation methods, respectively. The equilibration steps and production steps were 10<sup>5</sup>. *Ab initio* molecular dynamics simulations where the host and guests are considered to be robust and flexible were performed using the Dynamics task in the Dmol<sup>3</sup> module. The process adopted the canonical ensemble with constant volume/temperature (NVT) using a Nose-Hoover thermostat with a time step of 1.0 fs at 95 °C.

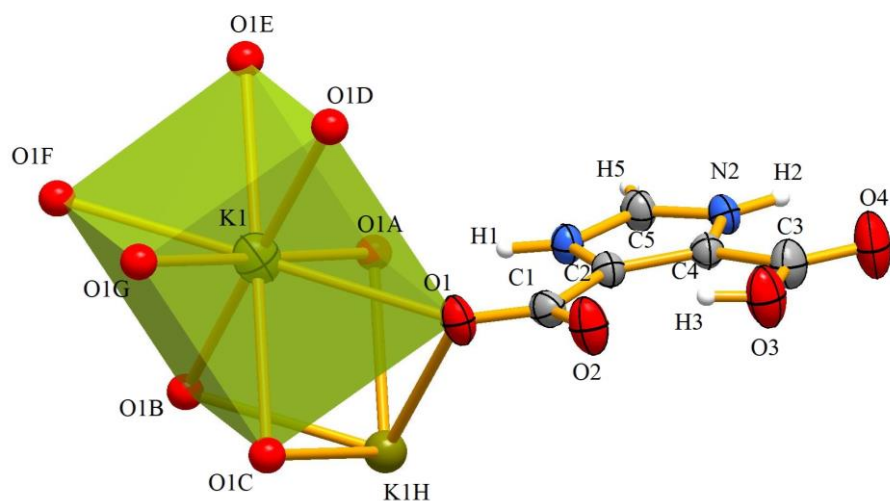


**Fig. S1** The coordination environment in **1**-H<sub>2</sub>O (Symmetry codes: A =  $3/4-y, -1/4+x, -1/4-z$ ; B =  $1-x, 1/2-y, z$ ; C =  $1/4+y, 3/4-x, -1/4-z$ ; D =  $x, y, 1+z$ ; E =  $3/4-y, -1/4+x, 3/4-z$ ; F =  $1-x, 1/2-y, 1+z$ ; G =  $1/4+y, 3/4-x, 3/4-z$ ; H =  $x, y, -1+z$ ).

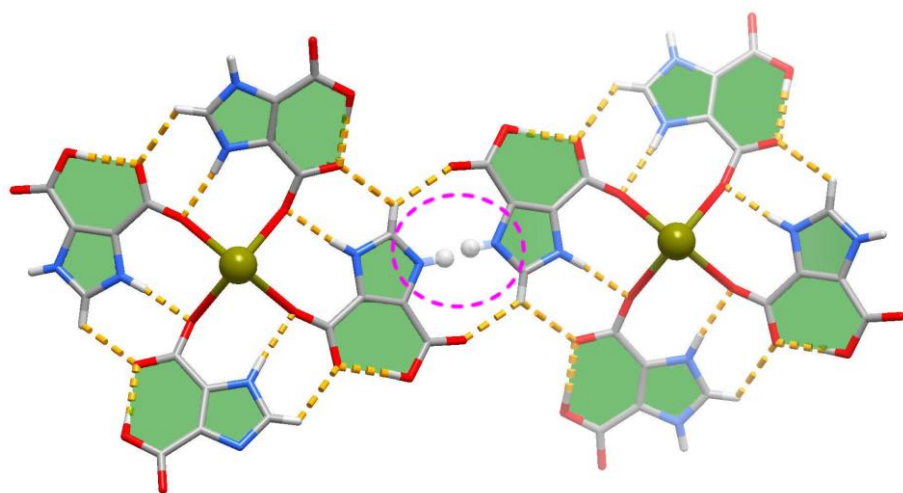


**Fig. S2** Two-fold disordered hydrogen atoms of imidazole groups in **1**-H<sub>2</sub>O.

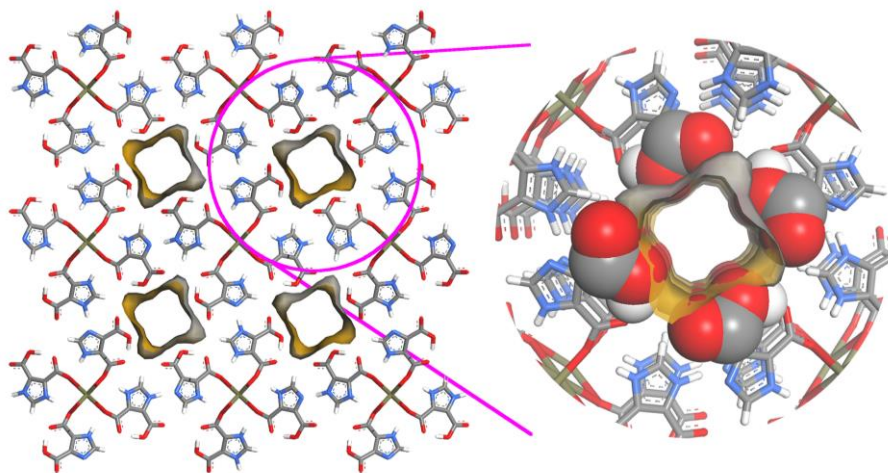


**Fig. S3** 1D pore channels studded with COOH/COO<sup>-</sup> groups in **1**.

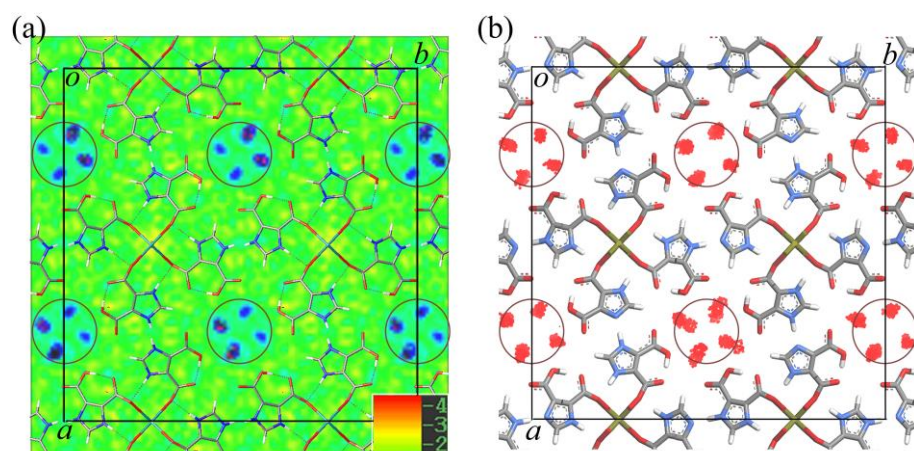


**Fig. S4** Locations of guests obtained from (a) SCXRD (electronic cloud) and (b) GCMC simulations (density field) along the *c*-axis in **1** (dots with distances shorter than 5 Å are enclosed in brown circles).

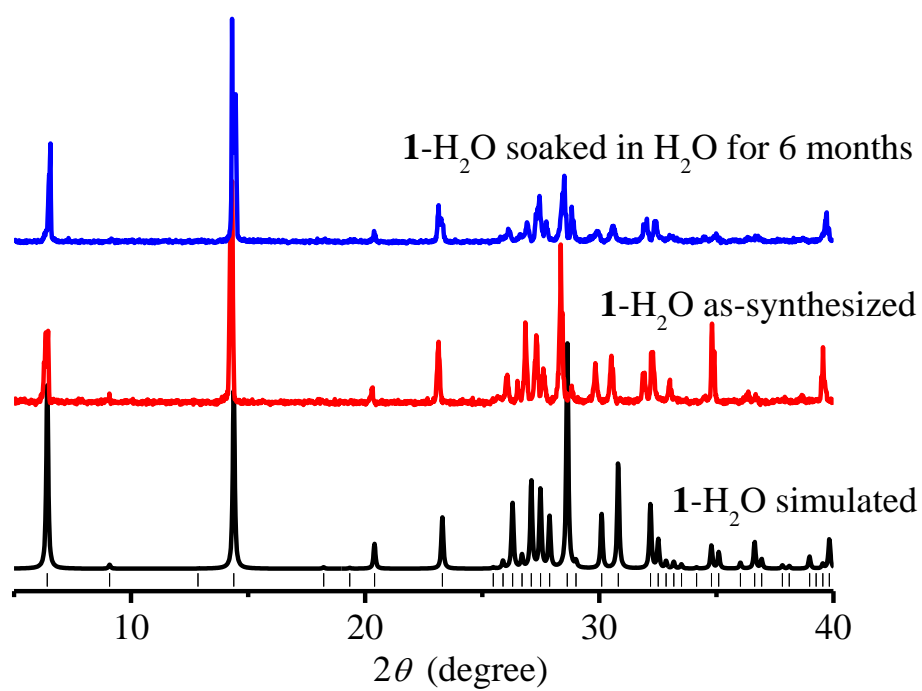


**Fig. S5** PXR D patterns of 1-H<sub>2</sub>O at different conditions.

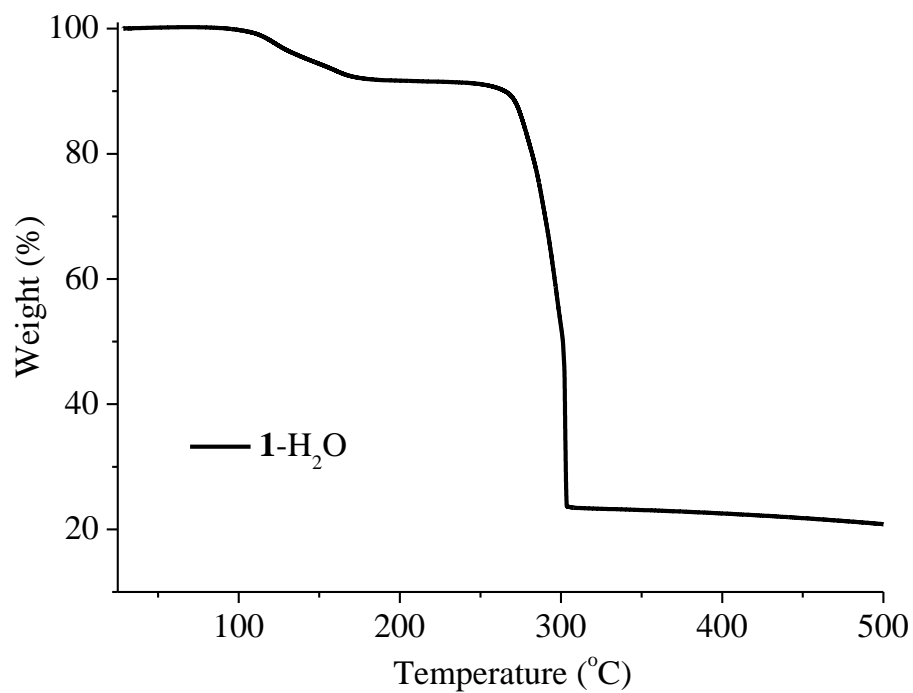


**Fig. S6** TG curve of 1-H<sub>2</sub>O.

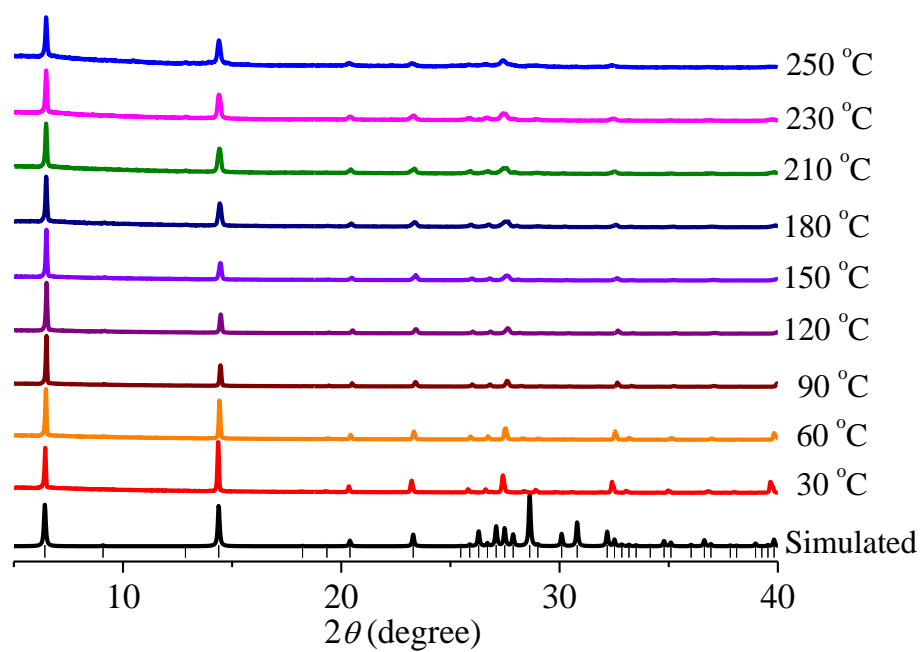


**Fig. S7** Variable-temperature PXRD patterns of 1-H<sub>2</sub>O.

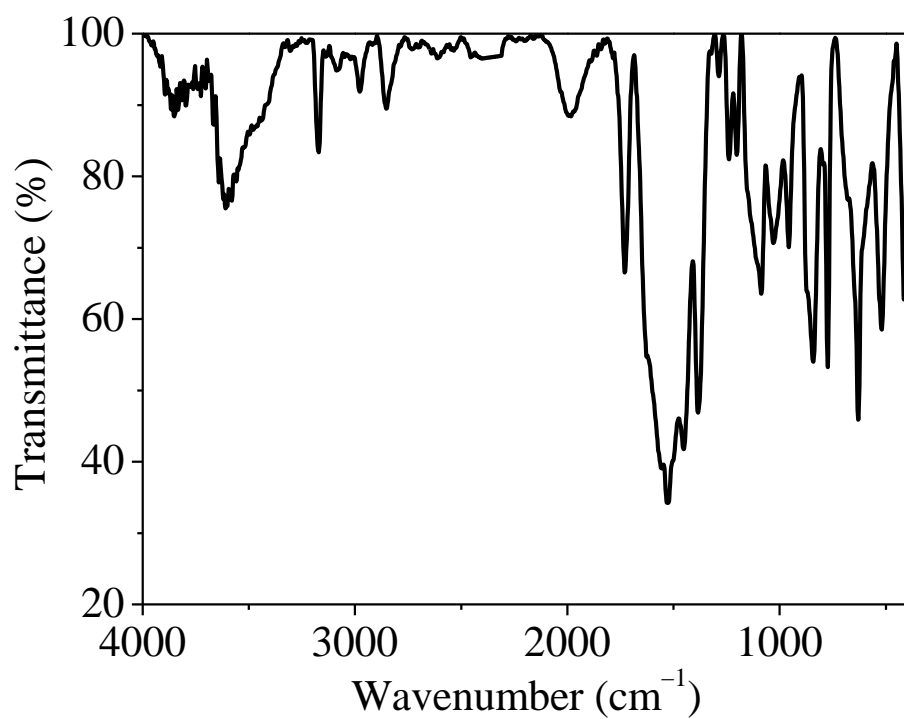


**Fig. S8** IR spectrum of 1-H<sub>2</sub>O. Broad peaks above 3300 cm<sup>-1</sup> indicative of dispersive H<sub>3</sub>O<sup>+</sup>/H<sub>2</sub>O guests.

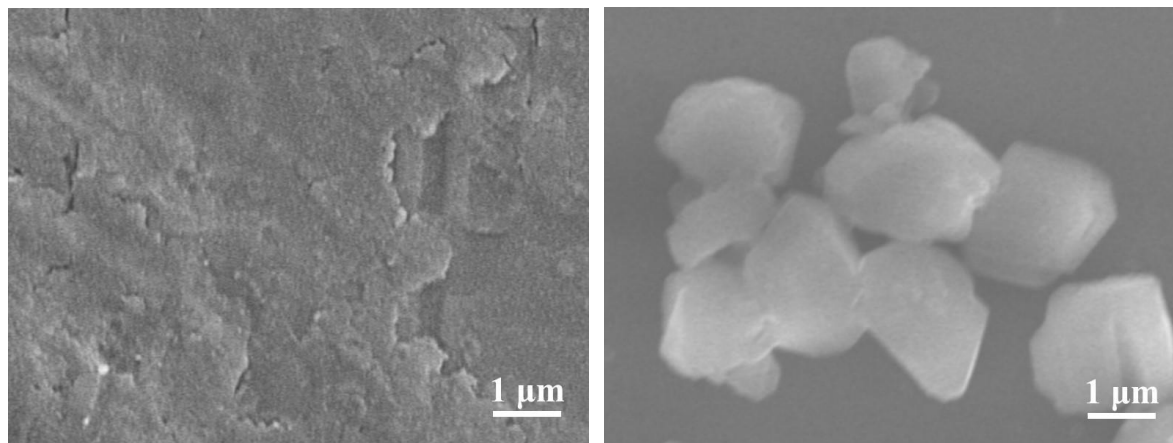


**Fig. S9** SEM images of pellet of **1-H<sub>2</sub>O**.

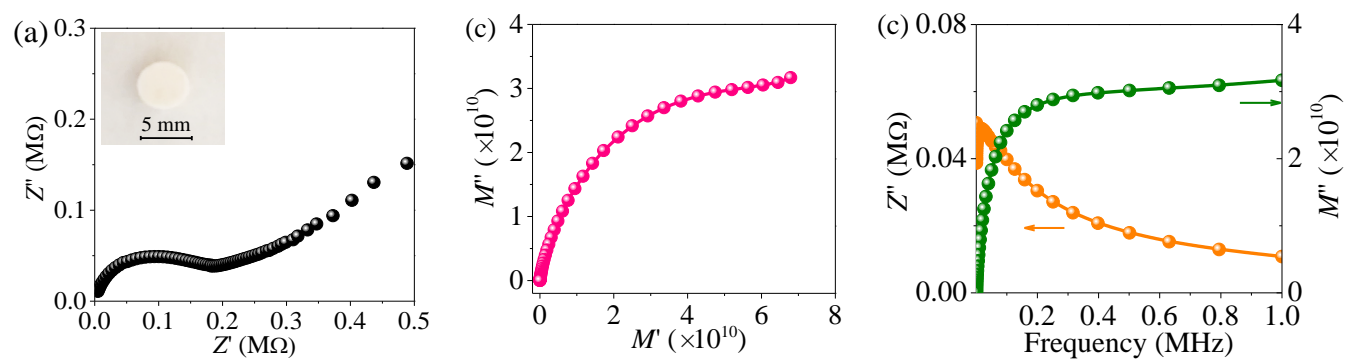


**Fig. S10** (a) Nyquist plots, (b) modulus plots, and (c)  $Z''$  and  $M''$  plots (versus frequency) for the pellet of **1-H<sub>2</sub>O** at 25 °C and 98% RH.



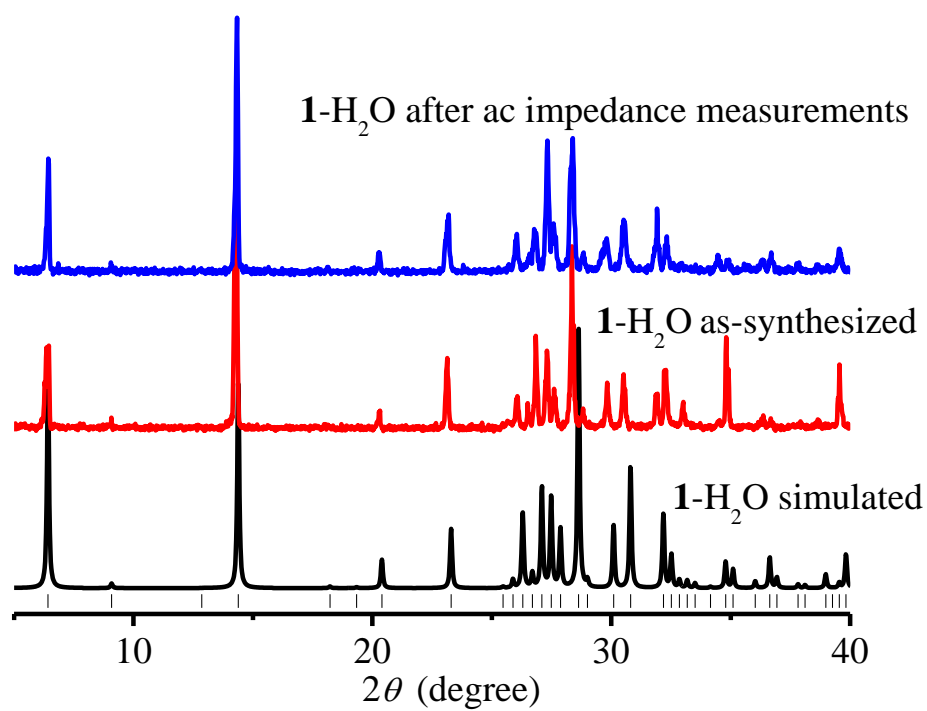


**Fig. S11** PXR D patterns of **1-H<sub>2</sub>O** after ac impedance measurements under 95 °C and 98% RH.

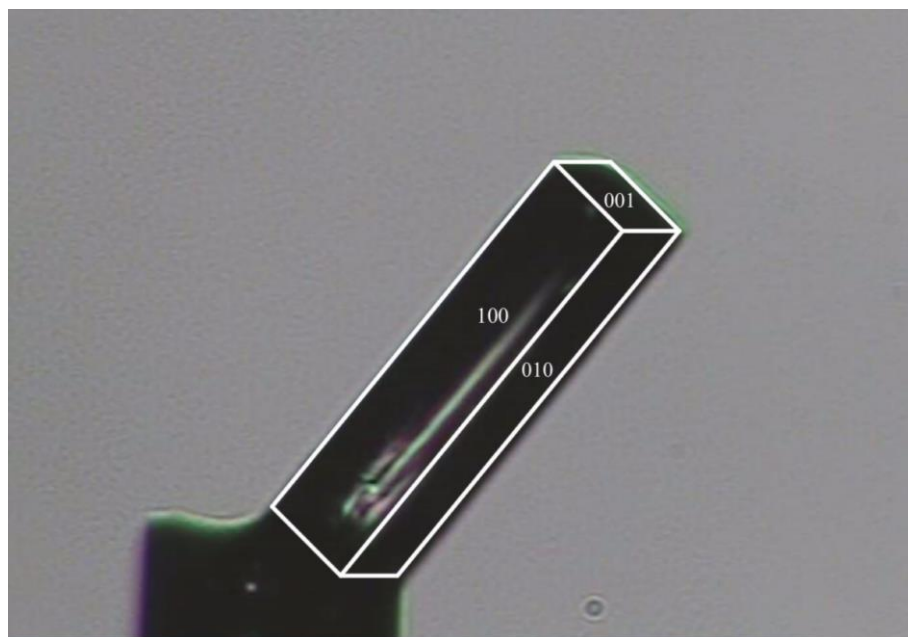


**Fig. S12** Determination for the crystal faces of **1-H<sub>2</sub>O**.

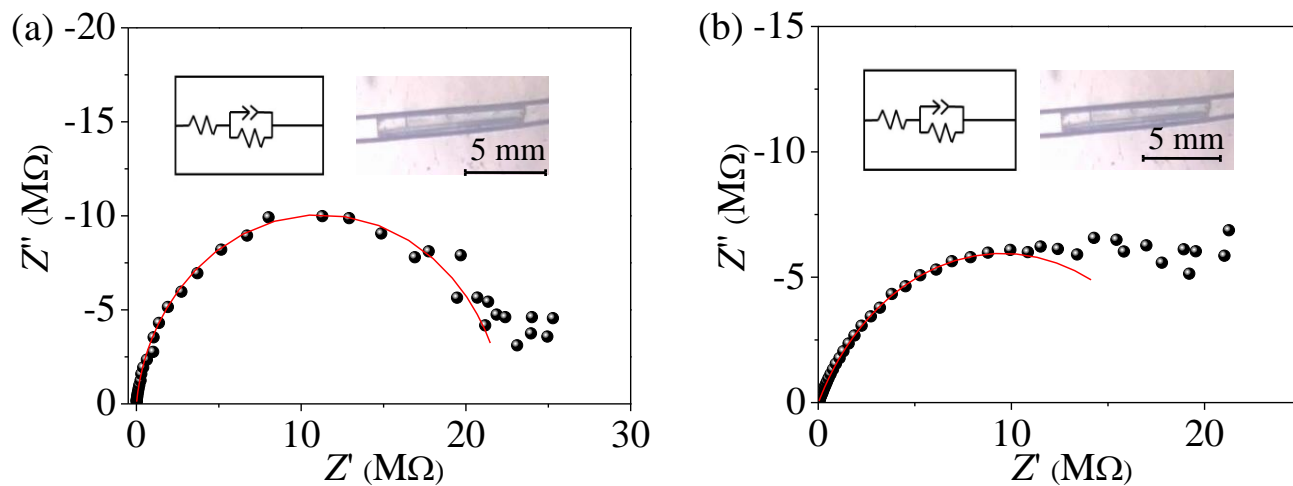


**Fig. S13** Nyquist plots for the single crystal of **1-H<sub>2</sub>O** measured perpendicularly to the {001} at (a) 25 °C and (b) 95 °C under 98% RH.

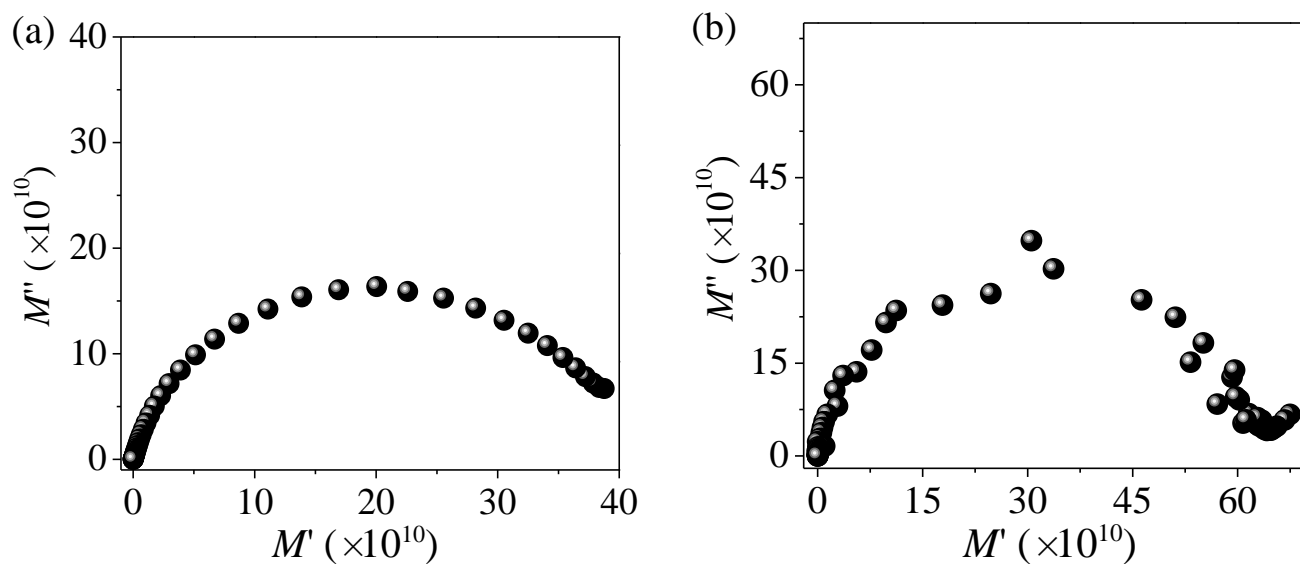


**Fig. S14** Modulus spectra for the single crystal of **1-H<sub>2</sub>O** measured (a) along and (b) perpendicularly to the {001} at 25 °C and 98% RH.

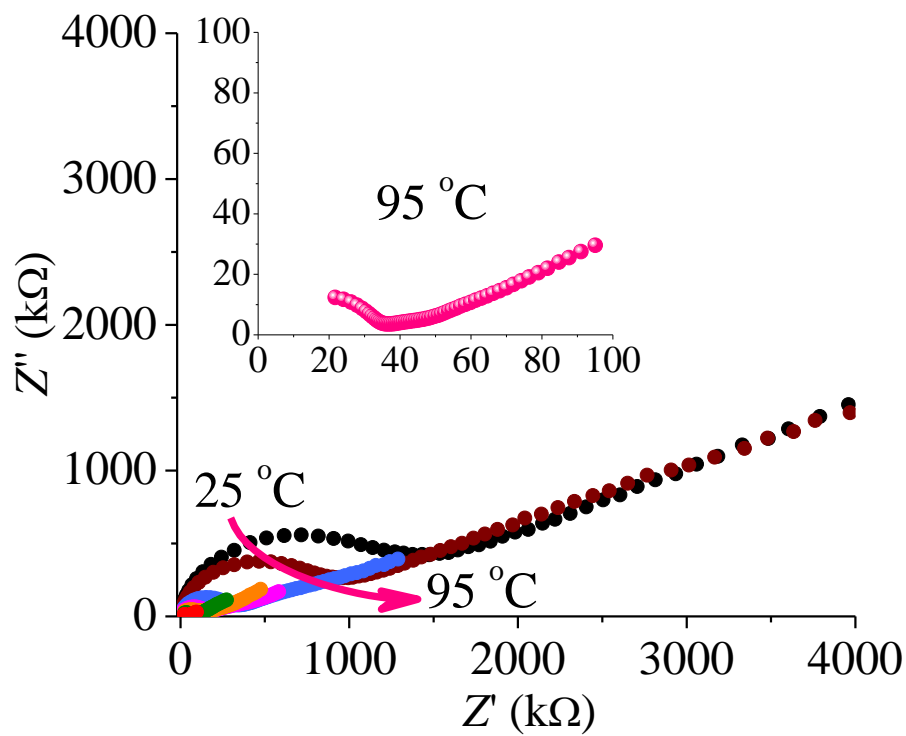


**Fig. S15** Nyquist plots of 1-H<sub>2</sub>O under 98% RH at different temperatures.

**Table S1.** Crystal data and structure refinement results.

Complex	<b>1-H<sub>2</sub>O</b>
Formula	C <sub>20</sub> H <sub>22</sub> KN <sub>8</sub> O <sub>19.5</sub>
Formula weight	725.55
Temperature (K)	150(2)
Crystal system	Tetragonal
Space group	<i>I</i> 4 <sub>1</sub> / <i>a</i>
<i>a</i> /Å	27.5128(5)
<i>c</i> /Å	3.52247(9)
<i>V</i> /Å <sup>3</sup>	2666.35(12)
<i>Z</i>	4
<i>D</i> <sub>c</sub> (g cm <sup>-3</sup> )	1.807
reflns coll.	9947
unique reflns	1094
Parameters	129
<i>R</i> <sub>int</sub>	0.0596
<i>R</i> <sub>1</sub> [ <i>I</i> > 2σ( <i>I</i> )] <sup>[a]</sup>	0.0656
<i>wR</i> <sub>2</sub> [ <i>I</i> > 2σ( <i>I</i> )] <sup>[b]</sup>	0.1703
<i>R</i> <sub>1</sub> (all data)	0.0755
<i>wR</i> <sub>2</sub> (all data)	0.1977
Completeness	0.998
GOF	1.027

<sup>a</sup>  $R_1 = \sum ||F_o| - |F_c|| / \sum |F_o|$ .

<sup>b</sup>  $wR_2 = [\sum w(F_o^2 - F_c^2)^2 / \sum w(F_o^2)^2]^{1/2}$ .

**Table S2.** Anisotropic proton conductivities of crystalline porous materials measured by single crystals.

Materials	$\sigma_{//}$ (S cm <sup>-1</sup> )	$\sigma_{\perp}$ (S cm <sup>-1</sup> )	Conditions	$E_a$ (eV)	Prominent guests	Pore features	Refs.
<b>1-H<sub>2</sub>O</b>	$1.2 \times 10^{-2}$	$1.1 \times 10^{-7}$	95 °C and 98% RH	0.54	H <sub>3</sub> O <sup>+</sup> and H <sub>2</sub> O	COOH/COO <sup>-</sup> groups onto the 1D channels	This work
<b>PCMOF-17</b>	$1.3 \times 10^{-3}$	$8.7 \times 10^{-5}$	25 °C and 40% RH	-	Me <sub>2</sub> NH <sub>2</sub> <sup>+</sup> and H <sub>2</sub> O	SO <sub>3</sub> H groups inside the 2D interlayer spaces	<i>J. Am. Chem. Soc.</i> <b>2017</b> , <i>139</i> , 7176
<b>CoCa 4H<sub>2</sub>O</b>	$1.0 \times 10^{-3}$	$4.4 \times 10^{-8}$	25 °C and 95% RH	0.90	ClO <sub>4</sub> <sup>-</sup> and H <sub>2</sub> O	Phosphonate groups and coordinated H <sub>2</sub> O inside the 2D interlayer spaces	<i>Chem. Mater.</i> <b>2015</b> , <i>27</i> , 8116
<b>Co-MOF-74</b>	$1.2 \times 10^{-2}$	$1.2 \times 10^{-3}$	25 °C and 92% RH	0.87	H <sub>2</sub> O	Coordinated H <sub>2</sub> O arranged along the 1D channels	<i>Nanomaterials</i> <b>2020</b> , <i>10</i> , 1263
<b>PCC-72</b>	$3.4 \times 10^{-3}$	$3.2 \times 10^{-4}$	22 °C and 99% RH	-	H <sub>2</sub> O	μ-OH groups onto the 3D pore channels	<i>Adv. Mater.</i> <b>2016</b> , <i>28</i> , 10772
<b>CFA-17</b>	$3.3 \times 10^{-3}$	$2.1 \times 10^{-5}$	22 °C and 94% RH	-	H <sub>2</sub> O	Triazolate, carbonyl groups and coordinated H <sub>2</sub> O onto the 1D channels	<i>ACS Appl. Nano Mater.</i> <b>2019</b> , <i>2</i> , 291
[Cu <sub>2</sub> (Htzehp) <sub>2</sub> (4,4'-bipy)] 3H <sub>2</sub> O	$1.4 \times 10^{-3}$	$2.5 \times 10^{-5}$	80 °C and 95% RH	0.48	H <sub>2</sub> O	OH groups arrayed inside the 2D interlayer spaces	<i>Chem. Mater.</i> <b>2017</b> , <i>29</i> , 2321
<b>Mg-NU-225</b>	$1.6 \times 10^{-3}$	$1.5 \times 10^{-5}$	55 °C and 95% RH	0.33	H <sub>2</sub> O	Phosphonate and carbonyl groups inside the 2D interlayer spaces	<i>Inorg. Chem.</i> <b>2021</b> , <i>60</i> , 1086